

ELECTRONIC SUPPLEMENTARY INFORMATION

Fluorescent cyclodextrin carriers for a water soluble Zn^{II}
pyrazinoporphyrazine octacation with photosensitizer potential

**R. Anand,¹ F. Manoli,¹ I. Manet,¹ M. P. Donzello,² E. Viola,² M. Malanga,³ L. Jicsinszky,³ E.
Fenyvesi,³ S. Monti^{1*}**

¹ *Istituto per la Sintesi Organica e la Fotoreattività, Consiglio Nazionale delle Ricerche ,
via P. Gobetti 101, I-40129 Bologna, Italy*

² *Dipartimento di Chimica, Università degli Studi di Roma “La Sapienza”,
P.le A. Moro 5, I-00185 Roma, Italy*

³ *CycloLab, Cyclodextrin R&D Ltd., Illatos út 7, H-1097 Budapest, Hungary*

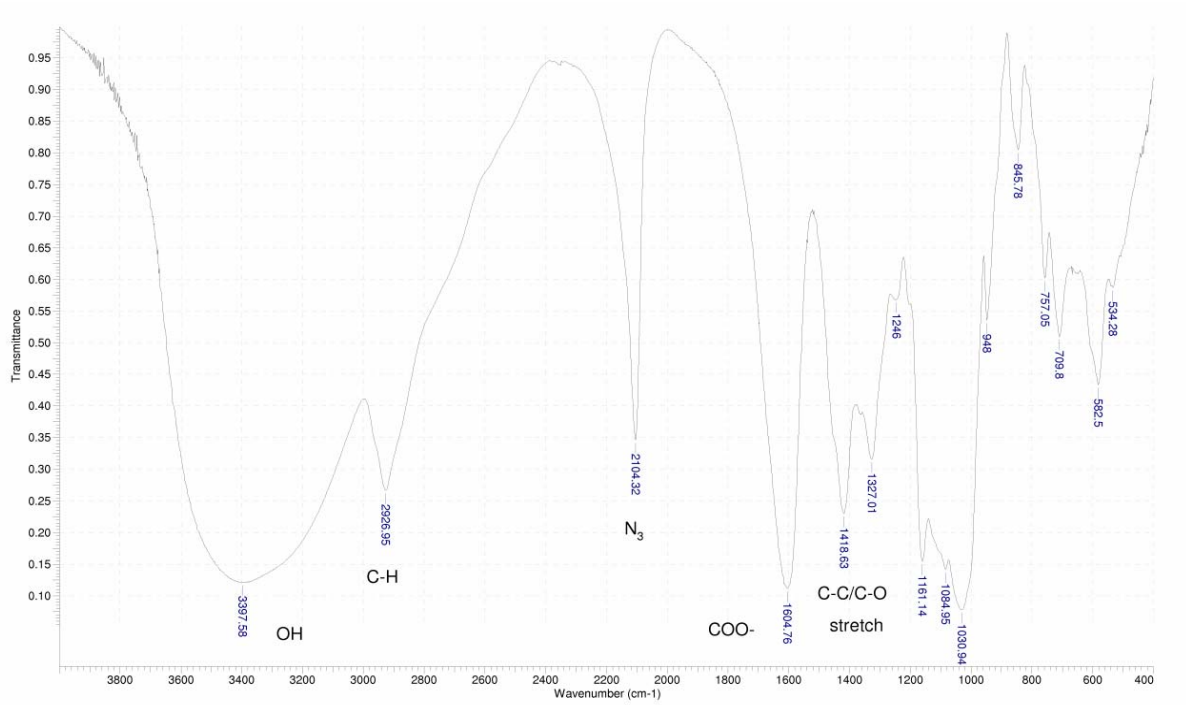
ESI-1. SPECTROSCOPIC DATA ON SYNTHESIZED MATERIALS

ESI-2. SELF-AGGREGATION OF $[(CH_3)_8LZn]^{8+}$

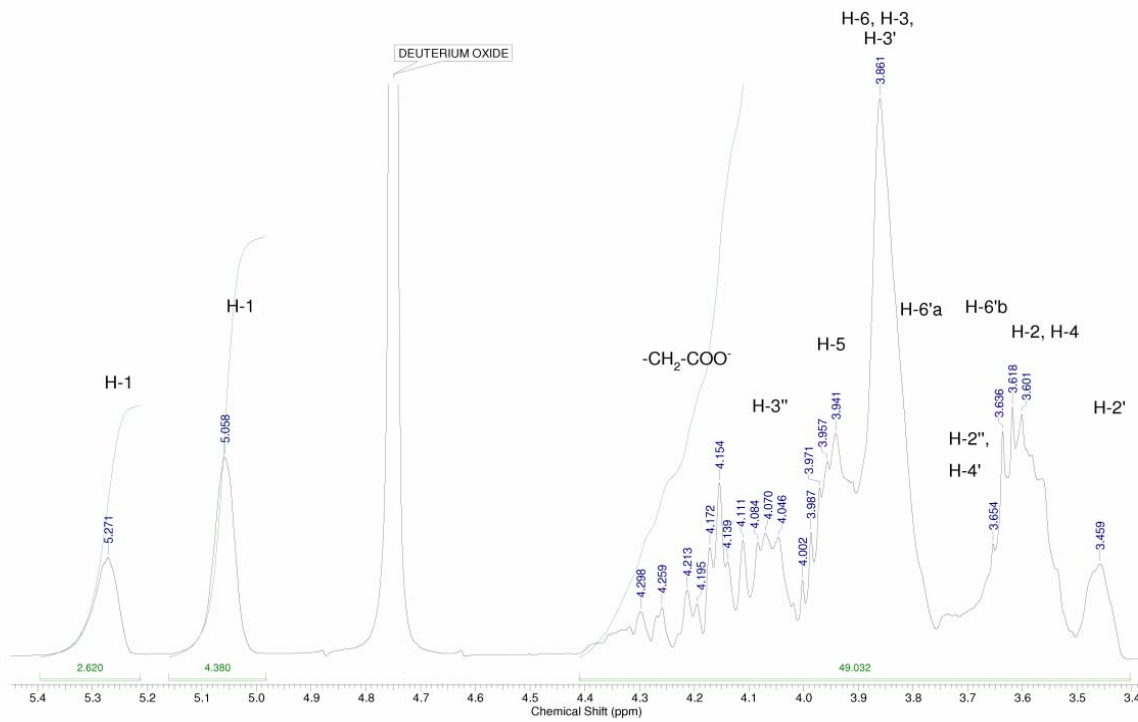
ESI-3 GLOBAL ANALYSIS OF EQUILIBRIUM SPECTROSCOPIC DATA

ESI-1. SPECTROSCOPIC DATA ON SYNTHESIZED MATERIALS

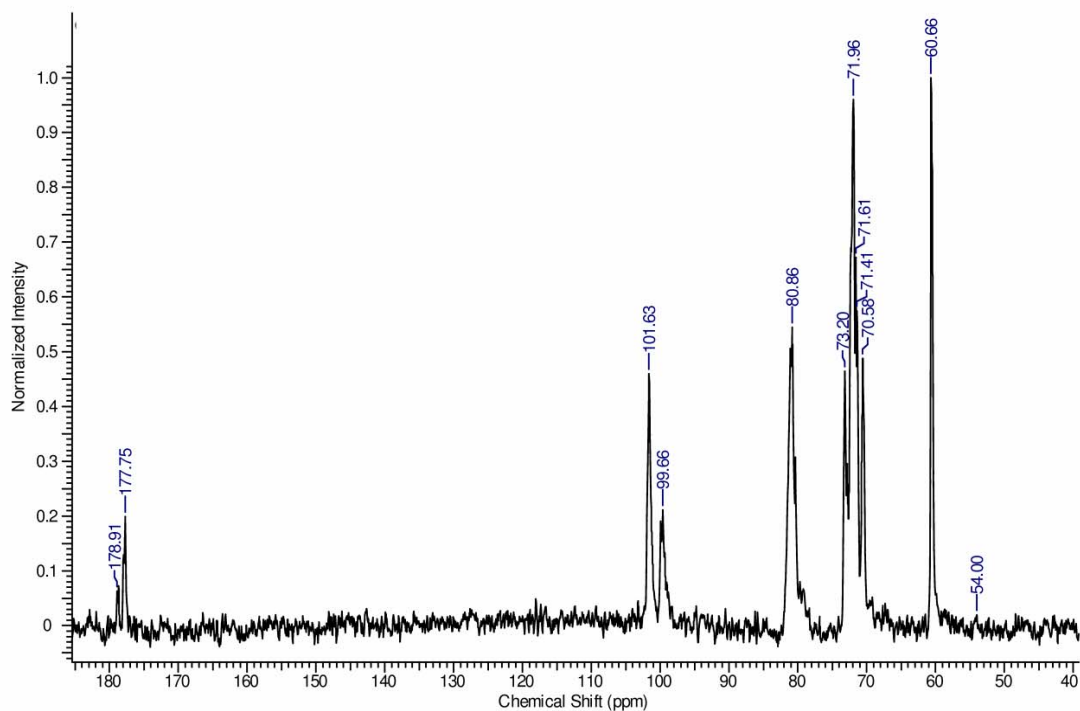
IR



¹H-NMR



¹³C-NMR



HSQC- DEPT

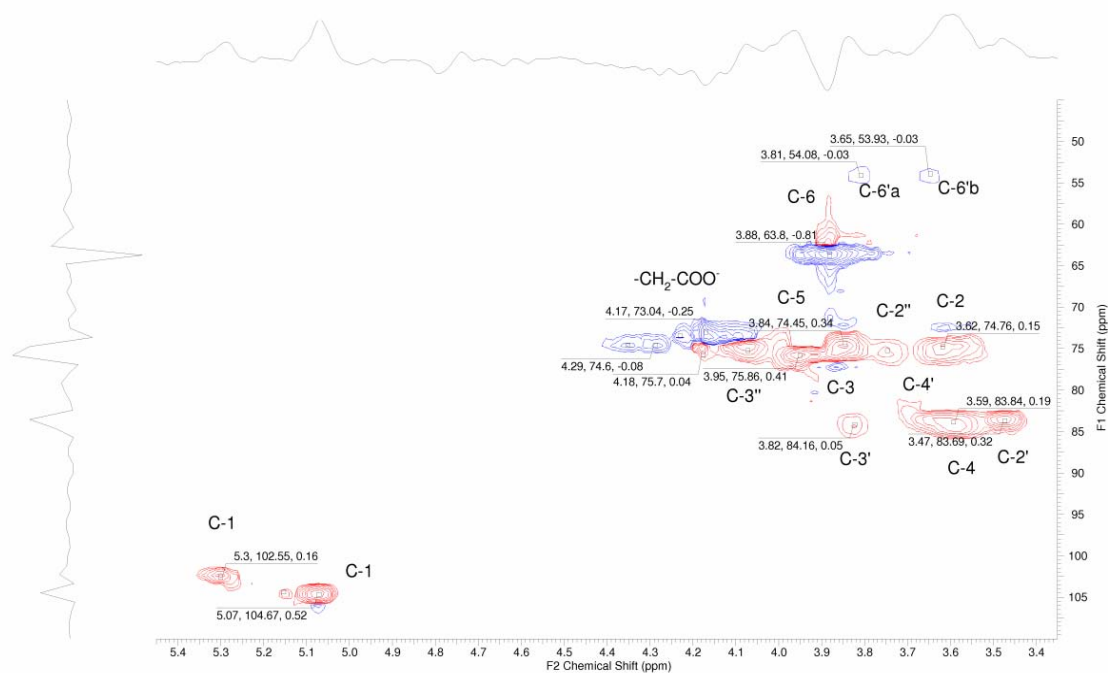
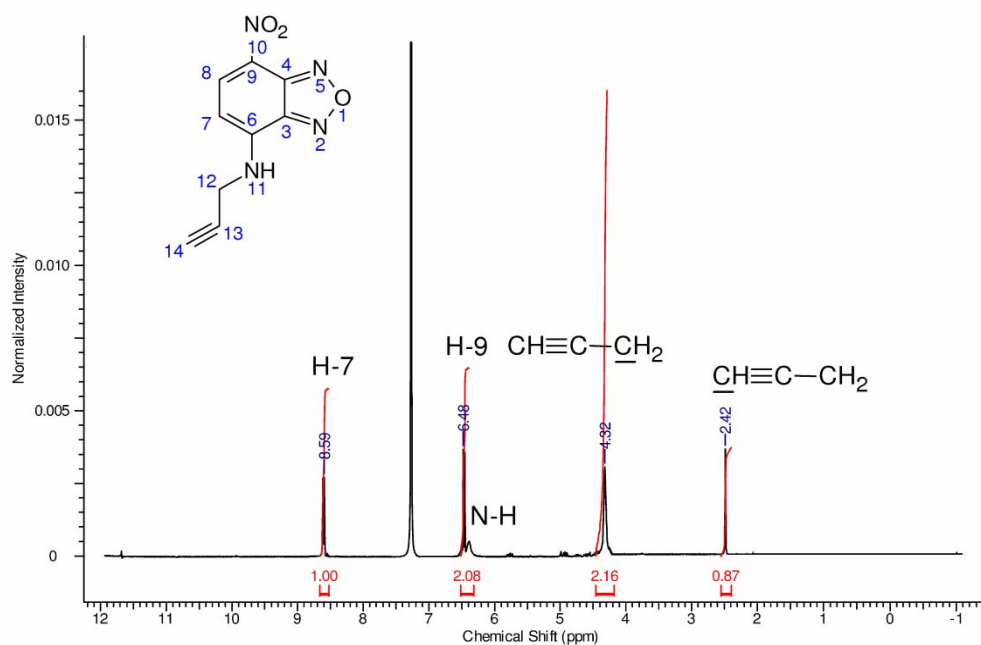


Figure S1. IR, ¹H-NMR, ¹³C-NMR and HSQC-DEPT of 6-monodeoxy-6-monoazido-carboxy-methyl- β -CyD sodium salt.

¹H-NMR



ESI-MS

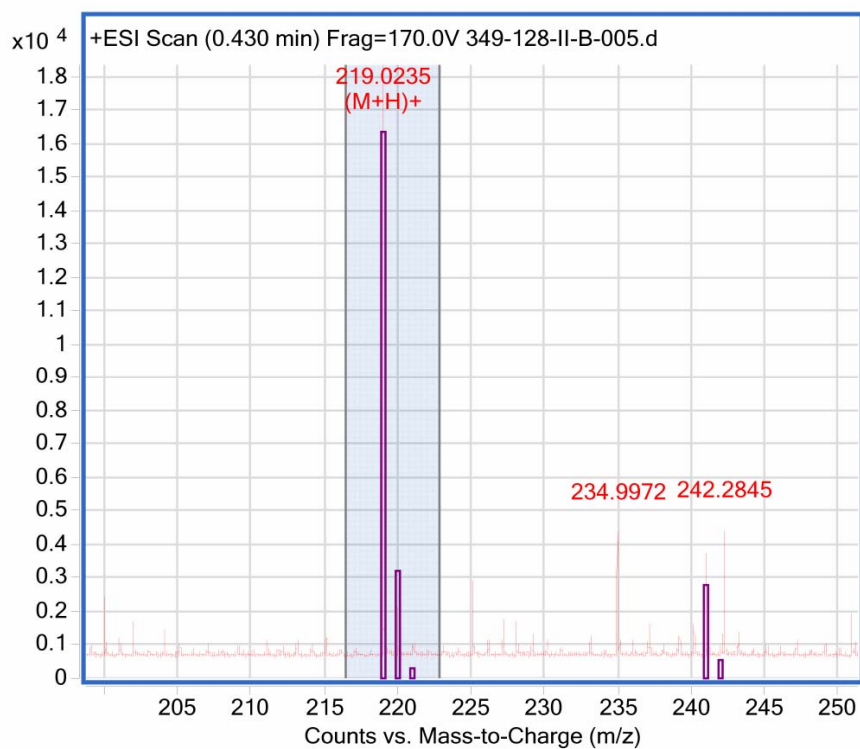
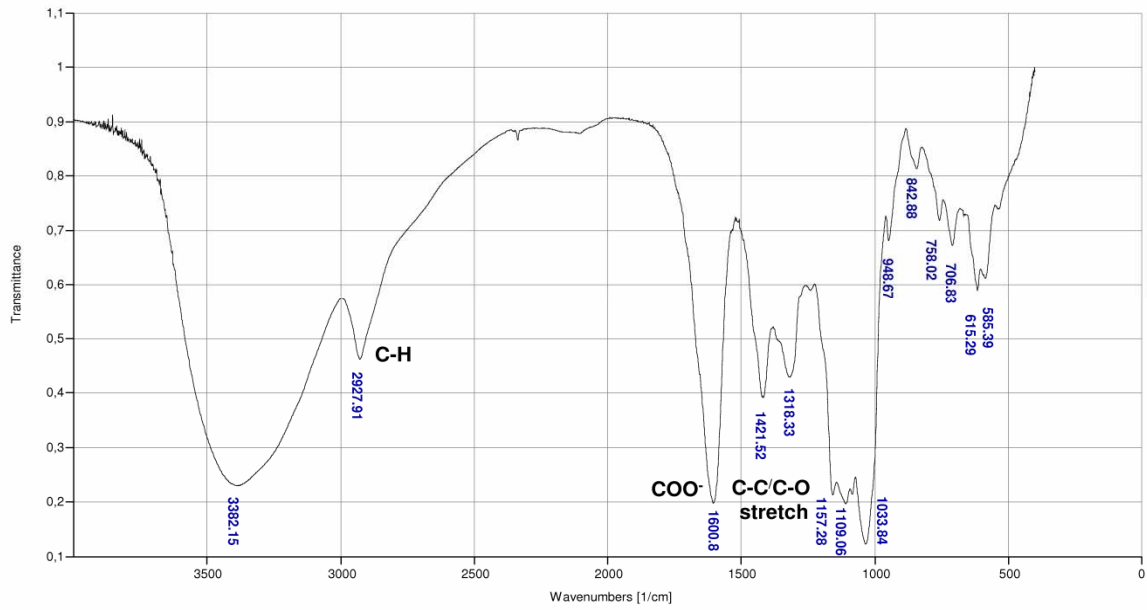
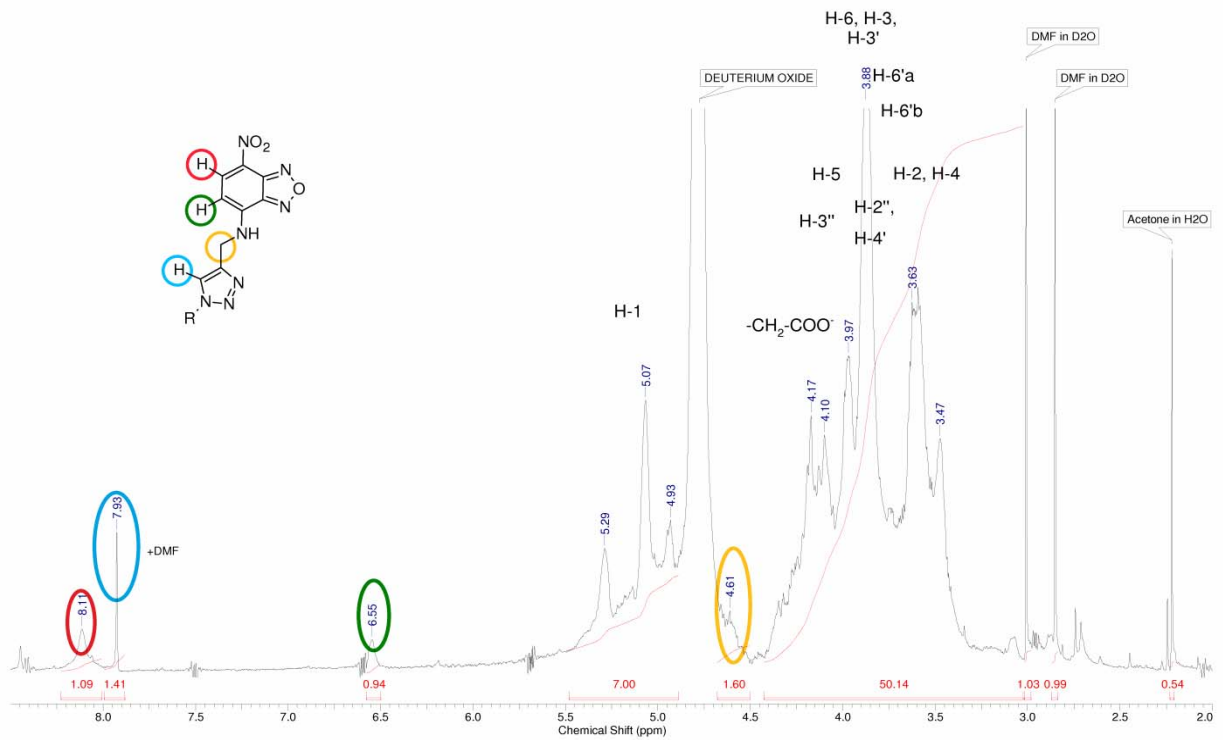


Figure S2: ¹H-NMR and ESI-MS of mono-4-(N-propargyl)-7-nitrobenzofuran.

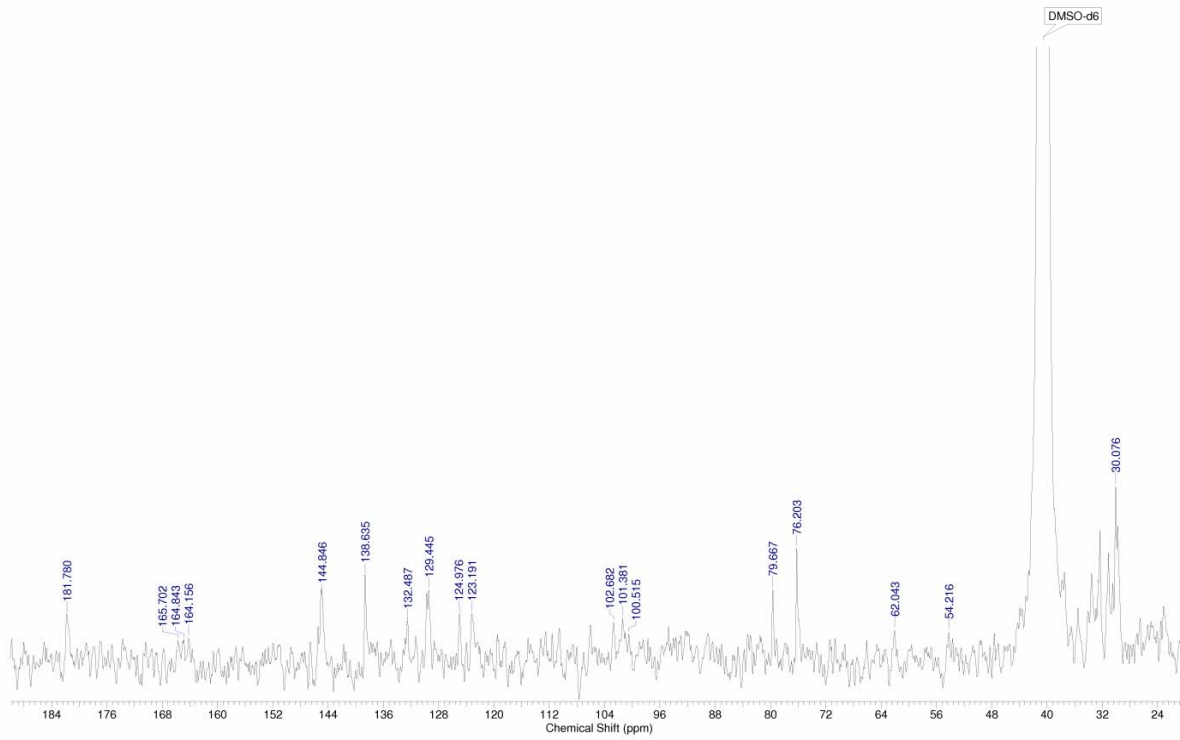
IR



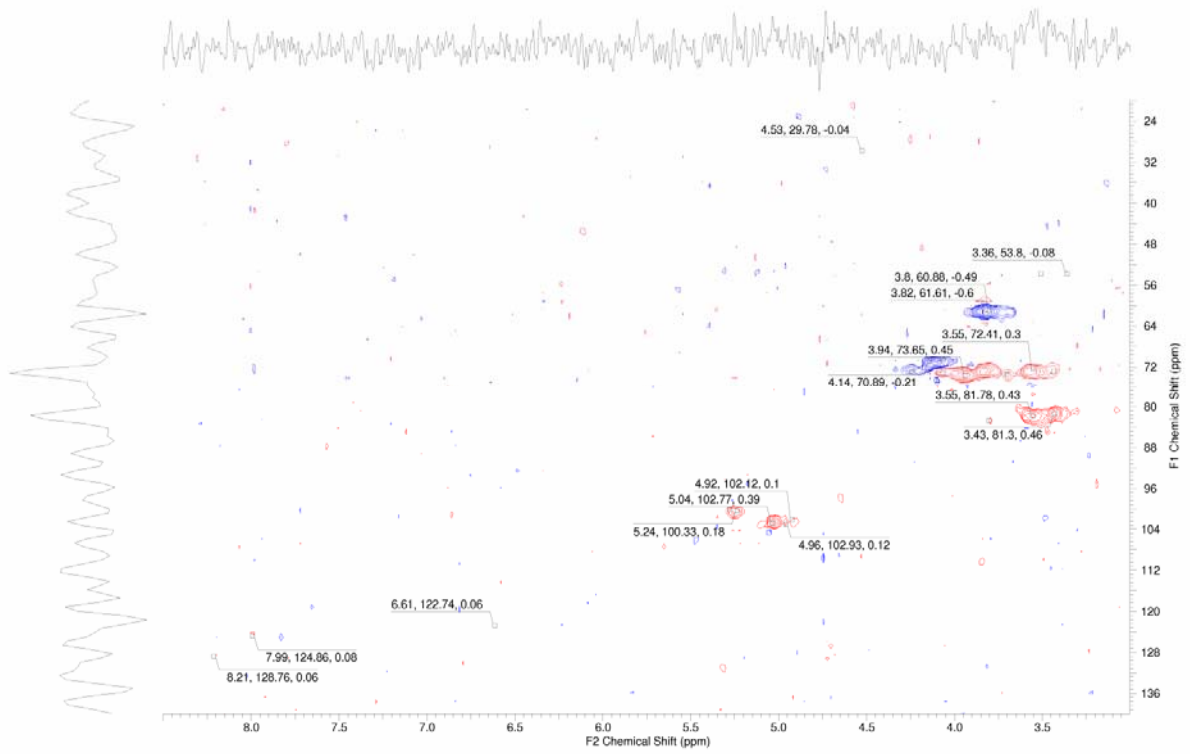
¹H-NMR



¹³C-NMR



HSQC-DEPT



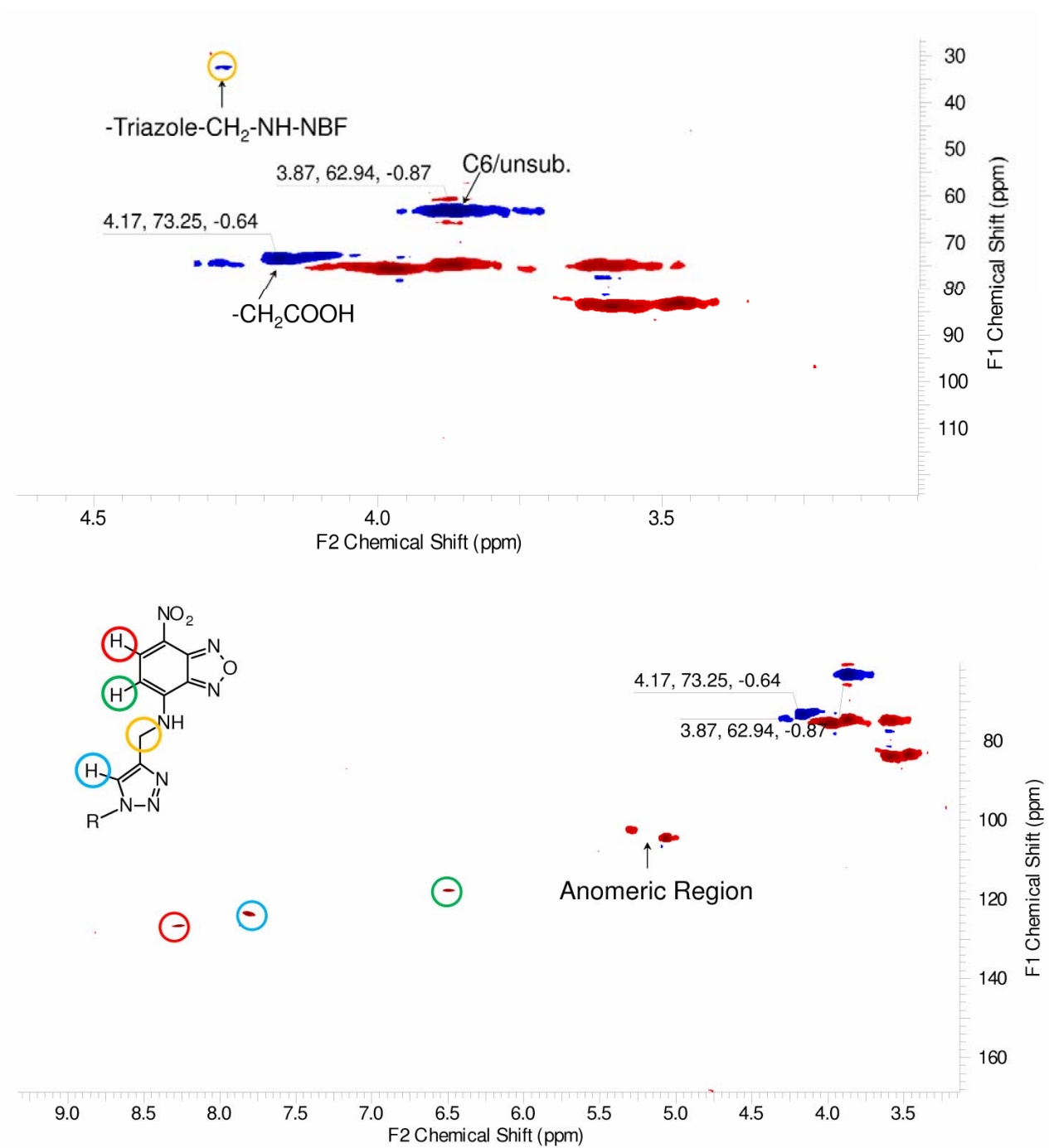


Figure S3 IR, ¹NMR, ¹³C-NMR and HSQC-DEPT spectra of nitrobenzofurazan-NH-triazolyl-carboxymethyl-β-CyD..

ESI-2. SELF-AGGREGATION OF $[(\text{CH}_3)_8\text{LZn}]^{8+}$

The UV-visible absorption spectrum of $[(\text{CH}_3)_8\text{LZn}]^{8+}$ in water (Figure S4) is characterized by a Q band system with two maxima of comparable intensity at ca. 625 and 655 nm, attributed to the dimer and monomer, respectively, in equilibrium with $\log(K_d/M^{-1}) = 7.1$.^{1,2} The broad envelope in the Soret region at 300-400 nm is composed of π, π^* transitions. The spectrum of the purely monomeric $[(\text{CH}_3)_8\text{LZn}]^{8+}$ was obtained in the presence of sodium dodecylsulfate (SDS) micelles.² It exhibits a dominating peak at ca. 660 nm, thanks to association of the octacationic macrocycle to the negatively charged micelle surface.

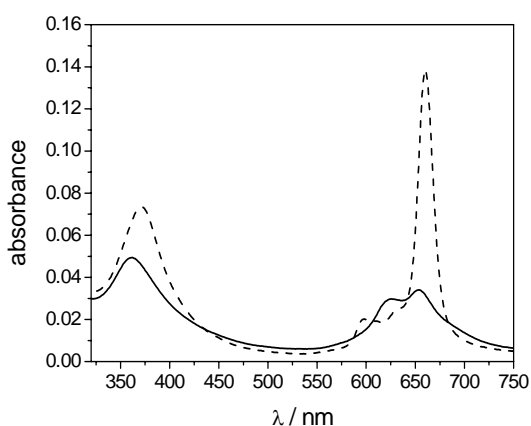


Figure S4. Absorption spectra of 1×10^{-6} M solution of $[(\text{CH}_3)_8\text{LZn}]^{8+}$ in water (solid line) and in water with 20 mM SDS (dashed line); cell path length 1.0 cm, 22 °C.

ESI-3. GLOBAL ANALYSIS OF EQUILIBRIUM SPECTROSCOPIC DATA

The receptor-ligand complexation equilibria were investigated by performing spectroscopic titrations. The best complexation model and the association constants were determined by multivariate global analysis of multiwavelength data from a series of spectra (UV-vis absorption, circular dichroism or fluorescence) corresponding to different mixtures, using the commercial SPECFIT/32 (v.3.0.40, TgK Scientific) program.^{3,4} Multiwavelength spectroscopic data sets (absorbances, ellipticities or fluorescence intensities) are arranged in matrix form \mathbf{Y} , where a

number N_w of wavelengths and a number N_m of corresponding measured spectroscopic signals are ordered in columns, whereas ligand and receptor concentrations are inserted in rows. Thus each element of the data matrix Y_{ij} corresponds to a wavelength j and an experimental quantity (absorbance, ellipticity or fluorescence intensity) for a given couple of concentrations i of ligand and receptor (typically in our experiments one of them is kept constant). A least square best estimator \mathbf{Y}' of the original data \mathbf{Y} is reconstructed as the eigenvector representation $\mathbf{Y}' = \mathbf{U} \times \mathbf{S} \times \mathbf{V}$, where \mathbf{S} is a vector that contains the relative weights of the significant eigenvectors (N_e , number of significant eigenvectors), \mathbf{U} is a matrix ($N_m \times N_e$) of concentration eigenvectors ($\mathbf{U}^T \times \mathbf{U} = 1$, orthonormal) and \mathbf{V} ($N_e \times N_w$) is a matrix of spectroscopic eigenvectors ($\mathbf{V} \times \mathbf{V}^T$, orthonormal). This \mathbf{Y}' matrix contains less noise than \mathbf{Y} because the SVD procedure can factor random noise from the principal components. This reconstructed data matrix \mathbf{Y}' is utilized in the global fitting instead of the original data matrix \mathbf{Y} . Complexation equilibria are solved assuming a complexation model (i.e. contemporary presence of a number of complexes of given stoichiometries in equilibrium with free species in solution) and optimizing the numeric combination of all the spectroscopic contributions ("colored" species) to best reproduce the \mathbf{Y}' signals. The analysis relies mainly to absorption data, but also CD and fluorescence data may be analysed, in the latter case provided they are relevant to optically thin samples (linear dependence of fluorescence signal on concentration for all the species involved). Given the direct linearity between experimental signal and concentration and the relation that must exist between the concentrations of the various species in the postulated simultaneous equilibria, the program calculates the conditional association constants and the spectra of the complexes based on a non linear least square fit, using the Levenberg-Marquardt algorithm, to best reproduce the experimental data for all the explored wavelengths and ligand-receptor concentration couples. The quality of the fits was evaluated on the basis of their Durbin-Watson (DW) factor and the relative error of fit. The DW test is very useful to check for the presence of auto-correlation in the residuals. This method is recommended for systematic misfit errors that can arise in titration experiments. It examines the tendency of successive residual errors to be correlated. The Durbin-

Watson statistics ranges from 0.0 to 4.0, with an optimal mid-point value of 2.0 for uncorrelated residuals (i.e. no systematic misfit). In contrast to the χ^2 (Chi-squared) statistics, which requires the noise in the experimental data is random and normally distributed, the DW factor is meaningful even when the noise level in the data set is low. Since the factorized data usually have a significantly lower noise level than the original data, DW test is ideal for the present type of data.

We applied this method to analyze UV-vis absorption, and FL titration experiments. Below, as an example, we describe the analysis of the UV-visible absorption changes of 8×10^{-6} M $[(\text{CH}_3)_8\text{LZn}]^{8+}$ upon titration with NBFT-CM β CyD from 1×10^{-6} M to 2×10^{-5} M at 22 °C (data of Figure 2 in the main text).

[FACTOR ANALYSIS]

Tolerance = 1.000E-09

Max.Factors = 10

Num.Factors = 7

Significant = 4

Eigen Noise = 2.586E-04

Exp't Noise = 2.586E-04

Eigenvalue Square Sum Residual Prediction

1 1.258E+02 5.952E-02 5.913E-03 Data Vector

2 4.991E-02 9.608E-03 2.377E-03 Data Vector

3 9.188E-03 4.201E-04 4.971E-04 Data Vector

4 3.066E-04 1.136E-04 2.586E-04 Data Vector

5 3.226E-05 8.133E-05 2.189E-04 Probably Noise

6 1.685E-05 6.448E-05 1.949E-04 Probably Noise

7 1.396E-05 5.053E-05 1.726E-04 Probably Noise

[SPECIES]	[COLORED]	[FIXED]	[SPECTRUM]
1 0 0	False	False	receptor
0 1 0	True	True	Monomer.FIX
0 2 0	True	True	Dimer.FIX
1 2 0	True	False	complex
2 2 0	True	False	complex

[SPECIES]	[FIXED]	[PARAMETER]	[ERROR]
1 0 0	True	0.00000E+00 +/-	0.00000E+00
0 1 0	True	0.00000E+00 +/-	0.00000E+00
0 2 0	True	7.10000E+00 +/-	0.00000E+00
1 2 0	False	1.33762E+01 +/-	5.26377E-01
2 2 0	False	1.94962E+01 +/-	4.57734E-01

[CONVERGENCE]

Iterations = 5

Convergence Limit = 1.000E-04

Convergence Found = 3.059E-05

Marquardt Parameter = 0.0

Sum(Y-y)² Residuals = 4.37462E-02

Std. Deviation of Fit(Y) = 5.06980E-03

[STATISTICS]

Experimental Noise = 2.586E-04

Relative Error Of Fit = 2.5789%

Durbin-Watson Factor = 1.3667

Goodness Of Fit, $\chi^2 = 3.844E+02$

Durbin-Watson Factor (raw data) = 1.3682

Goodness Of Fit, χ^2 (raw data) = None

[COVARIANCE]

5.571E+00 3.752E+00

3.752E+00 3.493E+00

[CORRELATION]

1.000E+00 8.504E-01

8.504E-01 1.000E+00

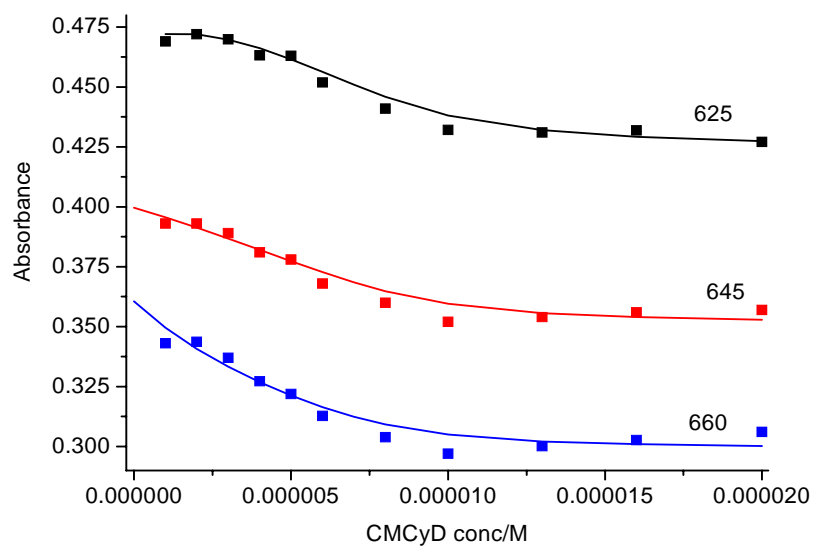


Figure S5. Global analysis of titration data of Figure 2 in the main text: comparison of experimental (symbols) and calculated (lines) absorbance at representative wavelengths (625, 645 and 660 nm), corresponding to $\log(K_{12}/M^2) = 13.4$ and $\log(K_{22}/M^3) = 19.5$ and spectra of the species in solution reported in Figure 4A of the main text.

References

1. I. Manet, F. Manoli, M. P. Donzello, E. Viola, G. Andreano, A. Masi, L. Cellai and S. Monti, *Org. Biomol. Chem.*, 2011, **9**, 684-688.
2. I. Manet, F. Manoli, M. P. Donzello, E. Viola, A. Masi, G. Andreano, G. Ricciardi, A. Rosa, L. Cellai, C. Ercolani and S. Monti, *Inorg. Chem.*, 2013, **52**, 321-328.
3. H. Gampp, M. Maeder, C. J. Meyer and A. D. Zuberbühler, *Talanta*, 1985, **32**, 257-264.
4. H. Gampp, M. Maeder, C. J. Meyer and A. D. Zuberbühler, *Talanta*, 1985, **32**, 95-101.